

Supplemental Material for "Convection self-aggregation in CNRM-CM6-1: equilibrium and transition sensitivity to surface temperature"

D. Coppin¹, R. Roehrig¹

¹Centre National de Recherches Météorologiques, Université de Toulouse, Météo-France, CNRS, Toulouse, France

Contents of this file

1. Text S1 to S9
2. Figures S1 to S9

Introduction The supplemental material provides additional figures designed to better understand the CRH distribution decomposition into two lognormal distribution and to more comprehensively document the aggregation mechanisms at the SSTs not investigated in details in the main manuscript.

Text S1. Figure S1 illustrates to what extent the sum of a dry and a moist lognormal distribution provides a good approximation of the full CRH distribution for three different time steps of the 305-K simulation.

Text S2. Figure S2 shows how the dry and moist CRH distribution components change with time. In this figure, we see that α , the fraction of the full distribution covered by

the moist component, decreases with time as the area below the moist curve becomes smaller than the one below the dry curve. The dry component becomes more peaked with time, which corresponds to a decrease in μ_d . Its skewness also increases towards the dry minimum meaning that σ_d increases with time. For the moist component, σ_m stays mostly constant while μ_m slightly decreases (more peaked distribution). Note that CRH_d and CRH_m , the CRH value at the dry and moist peaks, also change with time: CRH_d decreases and CRH_m increases. The dry and moist components intersect at CRH_c , which is used to distinguish between dry and moist regions.

Texts S3 and S4 Both figures S3 and S4 are similar to Figure 4 and show the relative humidity and cloud fraction profiles in the dry and moist regions separated at each time step by CRH_c , the CRH value where both dry and moist distribution are equal. The mean profile is an average over each day of the last year. It complements Figure 4 in the main manuscript.

Text S5 Figure S5 details the relative contributions of the clear-sky and cloudy-sky radiative feedbacks during the first 30 days of the 295-K, 300-K, 302-K and 305-K simulations. It complements Figure 7 in the main manuscript.

Texts S6 and S7 Figures S6 and S7 are the same as Figure 8 from the main manuscript but for the 300-K and 305-K simulations, respectively.

Text S8 Figure S8 details the clear-sky and cloudy-sky radiative feedbacks at 295 K. It complements Figure 8 in the main manuscript.

Text S9 Figure S9 shows the feedback decomposition for the 302-K simulation. It emphasizes the positive advection feedback that appears in the dry regions as in the simulation at 305 K but later (around day 150 here) while most other feedbacks remain constant after day 20. Equilibrium is reached around day 250. This figure complements Figure 12 in the main manuscript.

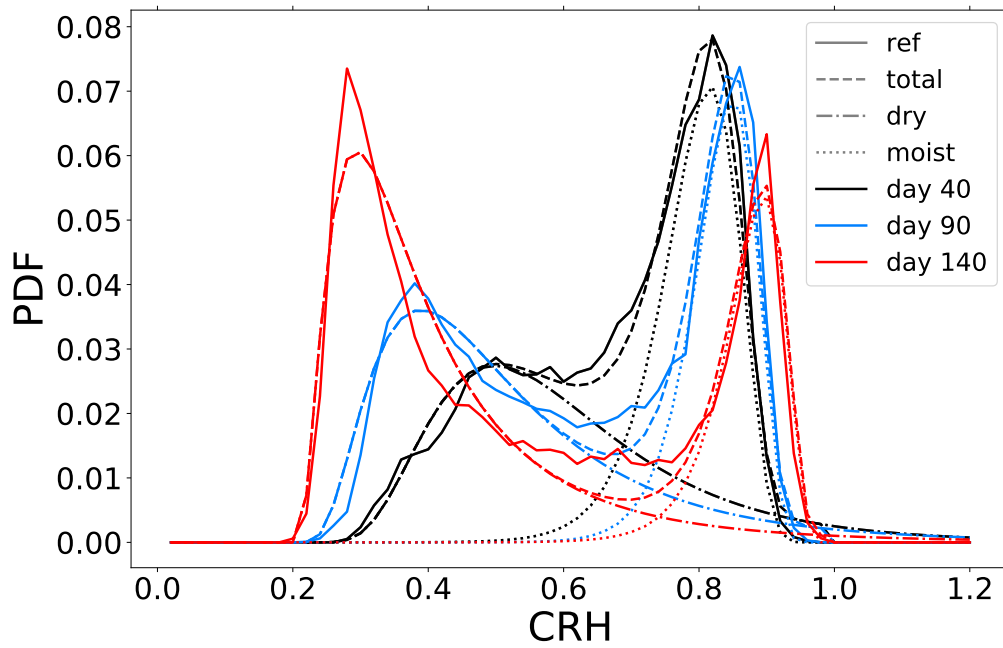


Figure S1. Probability density function of CRH at day 40 (black), day 90 (blue) and day 140 (red) for the 305 K simulation. For each day, the CRH distribution is shown with full line, while its dry and moist lognormal components are shown in dash-dotted and dotted lines, respectively. The sum of the dry and moist lognormal components is shown with dashed lines. See Equation 4 for details.

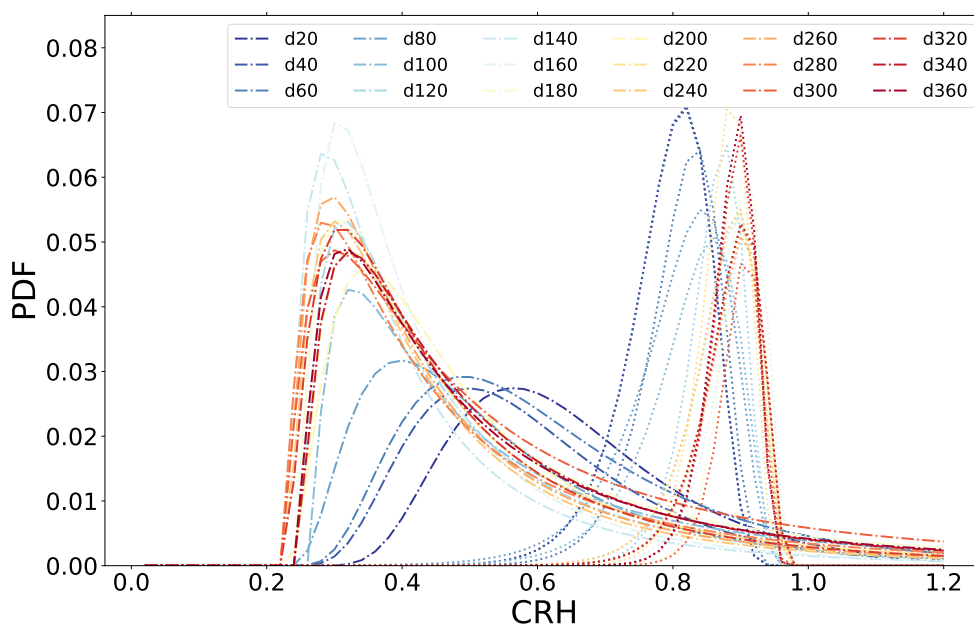


Figure S2. Dry (dash-dotted lines) and moist (dotted lines) components of the CRH probability distribution function estimated by Equation 4 every 20 days of the 305 K simulation. The colors from dark blue to dark red indicate increasing days at which the distributions are plotted.

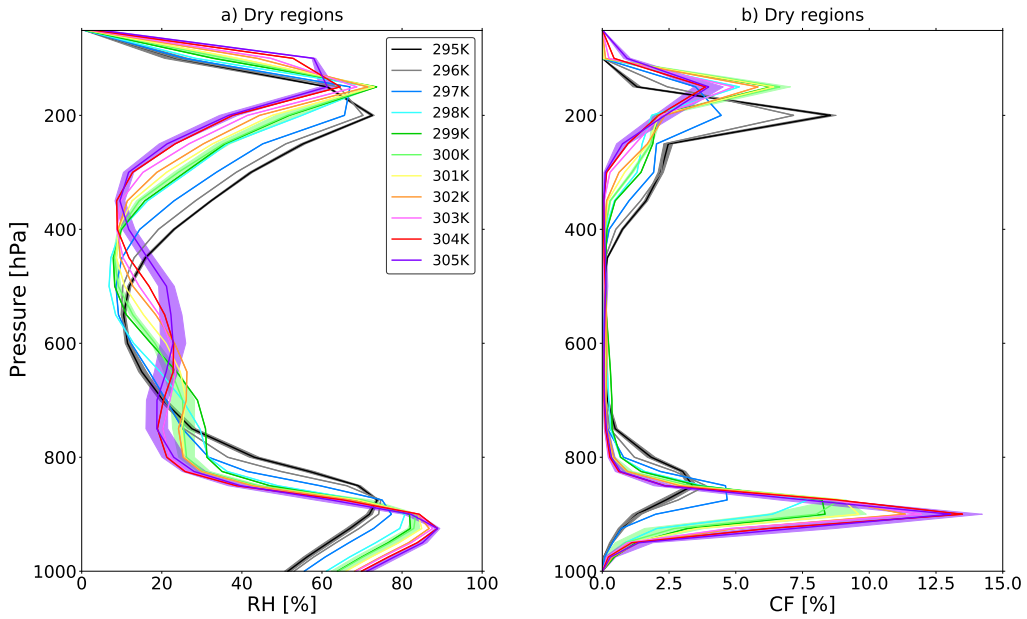


Figure S3. Mean profile of (a) relative humidity (RH, in %) and (b) cloud fraction (CF, in %) in the dry regions of all simulations (colored lines). Dry regions are identified as regions where CRH is lower than CRH_c . The shading indicates the 3-standard-deviation envelope of the 295-K, 300-K and 305-K ensembles. The time average is performed over the last year of each 3-year simulation.

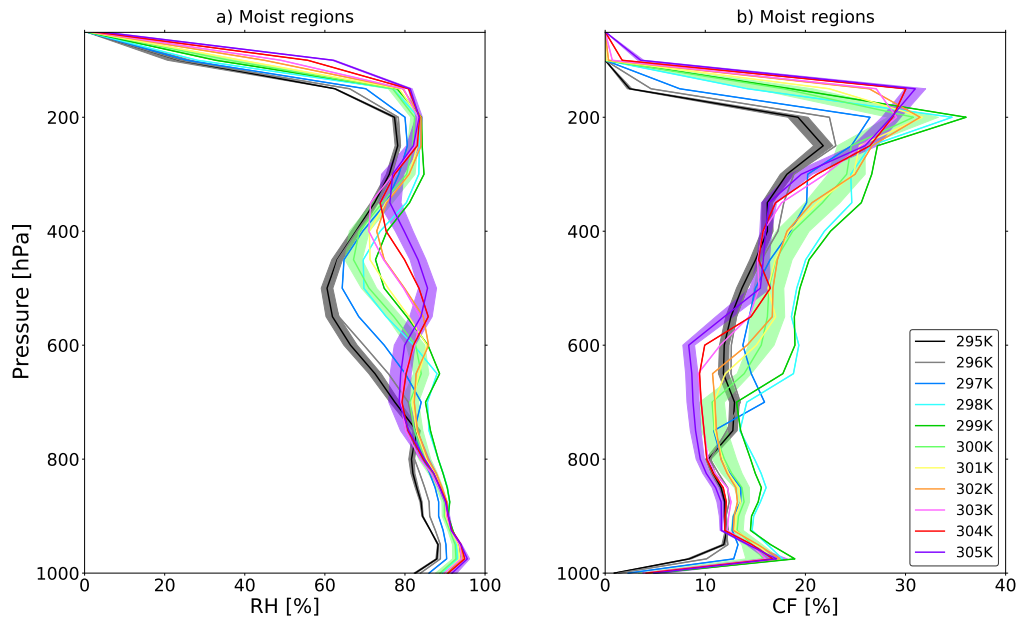


Figure S4. Mean profile of (a) relative humidity (RH, in %) and (b) cloud fraction (CF, in %) in the moist regions of all simulations (colored lines). Moist regions are identified as regions where CRH is higher than CRH_c . The shading indicates the 3-standard-deviation envelope of the 295-K, 300-K and 305-K ensembles. The time average is performed over the last year of each 3-year simulation.

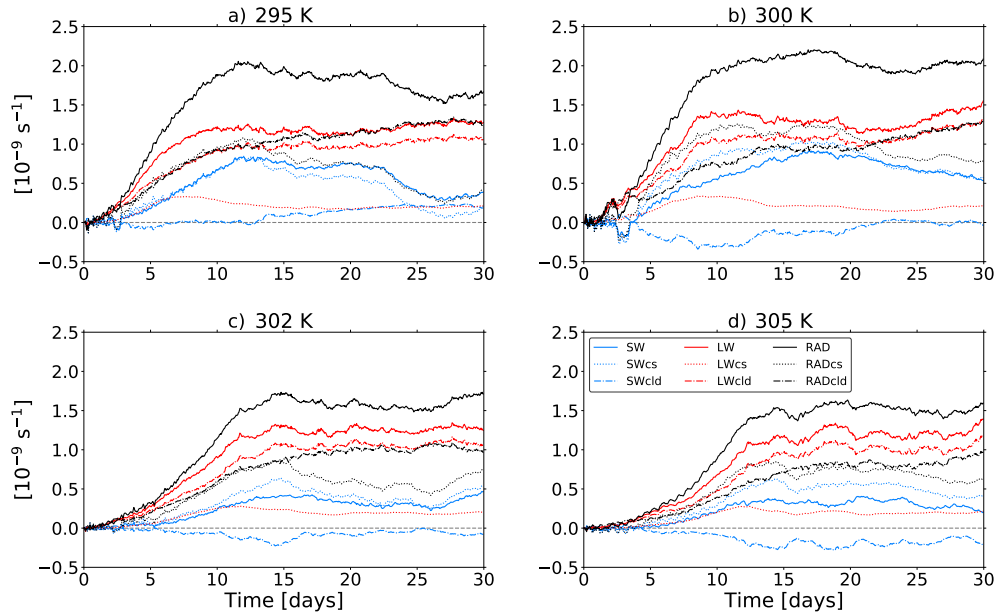


Figure S5. Time evolution of the shortwave (blue), longwave (red) and total (RAD = LW+SW, black) radiation feedbacks on the \hat{h}_n variance (in 10^{-9} s^{-1}) for the first 30 days of the (a) 295-K, (b) 300-K, (c) 302-K and (d) 305-K simulations. For each feedback, the clear-sky, cloudy-sky and total components are indicated with dotted, dash-dotted and solid lines, respectively.

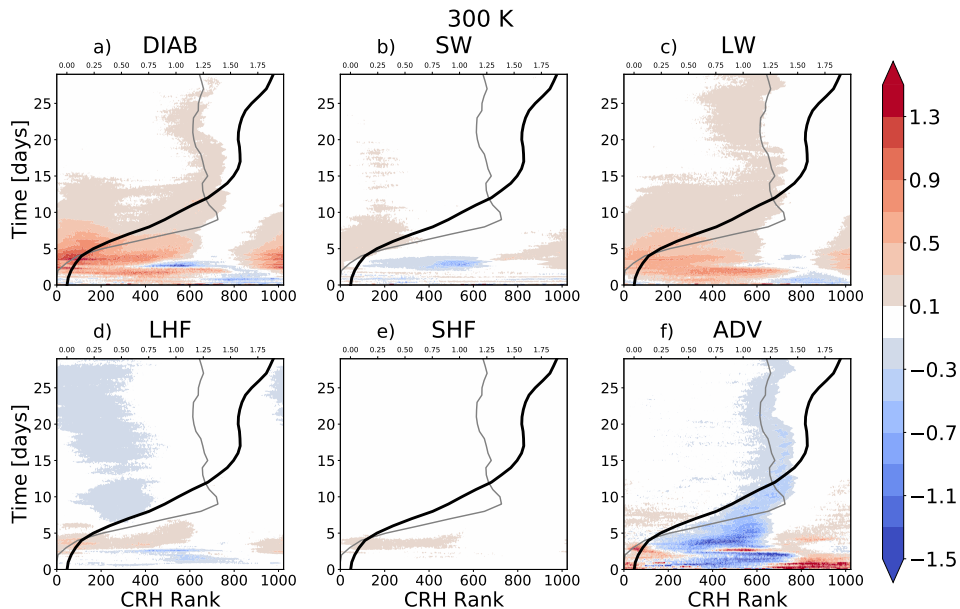


Figure S6. Time evolution of the (a) diabatic (DIAB = SW + LW + LHF + SHF) (b) shortwave (SW), (c) longwave (LW), (d) latent heat flux (LHF), (e) sensible heat flux (SHF), and (f) advection (ADV) feedbacks on the \hat{h}_n variance (in day^{-1}) for the first 30 days of the 300-K simulation and ranked according to the column relative humidity CRH. Feedbacks are normalized at each time step by the corresponding spatial variance of \hat{h}_n . The advection feedback is calculated using hourly model outputs. The black and grey solid lines indicate the time evolution of \hat{h}_n variance (in 10^{-3} , see upper x -axis for its scale) and the CRH rank corresponding to CRH_c , respectively.

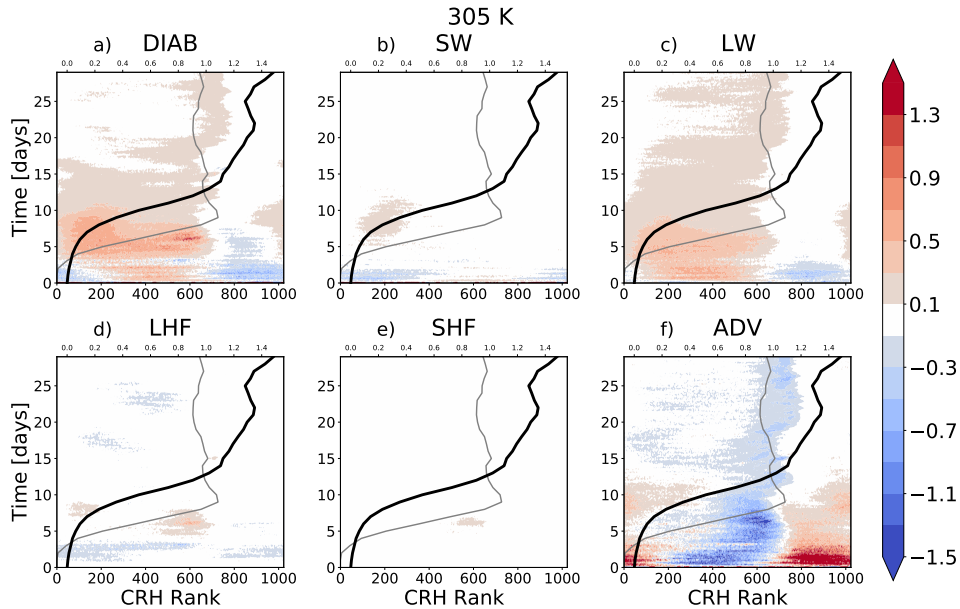


Figure S7. Time evolution of the (a) diabatic (DIAB = SW + LW + LHF + SHF) (b) shortwave radiation (SW), (c) longwave radiation (LW), (d) latent heat flux (LHF), (e) sensible heat flux (SHF), and (f) advection (ADV) feedbacks on the \hat{h}_n variance (in day^{-1}) for the first 30 days of the 305-K simulation and ranked according to the column relative humidity CRH. Feedbacks are normalized at each time step by the corresponding spatial variance of \hat{h}_n . The advection feedback is calculated using hourly model outputs. The black and grey solid lines indicate the time evolution of \hat{h}_n variance (in 10^{-3} , see upper x -axis for its scale) and the CRH rank corresponding to CRH_c , respectively.

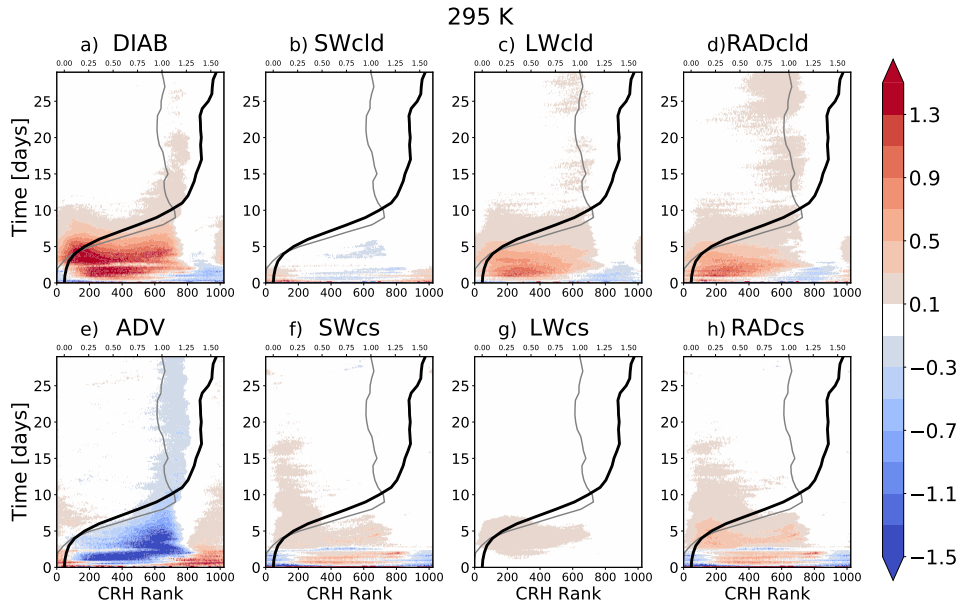


Figure S8. Time evolution of the (a) diabatic (DIAB = SW + LW + LHF + SHF), (b) cloudy-sky shortwave radiation (SWcld), (c) cloudy-sky longwave radiation (LWcld), (d) cloudy-sky radiation (RADcld = LWcld + SWcld), (e) advection (ADV), (f) clear-sky shortwave radiation (SWcs), (g) clear-sky longwave radiation (LWcs) and (h) clear-sky radiation (RADcs = LWcs + SWcs) feedbacks on the \hat{h}_n variance (in day^{-1}) for the first 30 days of the 295 K simulation and ranked according to the column relative humidity CRH. Feedbacks are normalized at each time step by the corresponding spatial variance of \hat{h}_n . The advection feedback is calculated using hourly model outputs. The black and grey solid lines indicate the time evolution of \hat{h}_n variance (in 10^{-3} , see upper x -axis for its scale) and the CRH rank corresponding to CRH_c , respectively.

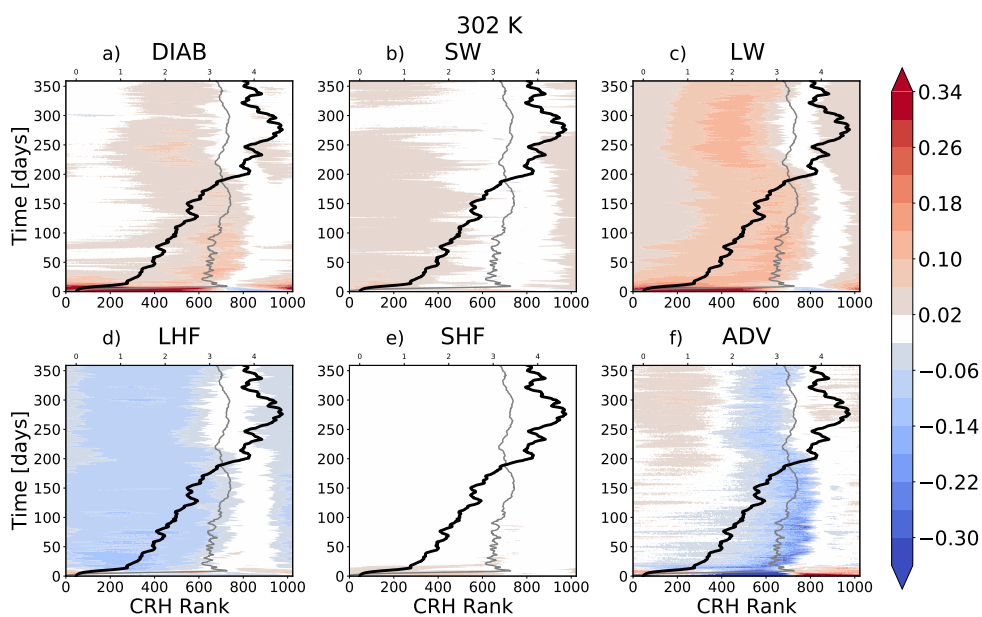


Figure S9. Same as Figure 12 (or S6 or S7) but for the first 360 days of the 302-K simulation.